Science of the Total Environment 868 (2023) 161376

Contents lists available at ScienceDirect

Science of the Total Environment

journal homepage: www.elsevier.com/locate/scitotenv

# Techno-economic evaluation of UV light technologies in water remediation

Deva Pelayo [a], María J. Rivero [a], Germán Santos [b], Pedro Gómez [b], Inmaculada Ortiz [a,*]

[a] Departamento de Ingenierías Química y Biomolecular, Universidad de Cantabria, Avda. Los Castros, s/n, 39005 Santander, Spain
[b] APRIA Systems, S.L., Bussines Park of Morero, Parcel P-2-12, Industrial Unit 1-Door 5, 39611 Guarnizo, Spain

## HIGHLIGHTS

- Photo-degradation of two CECs under UV irradiation dose typical of disinfection.
- UV-A/$TiO_2$ and UV-C/NaOCl provided the best results in terms of degradation kinetics.
- UV-C and UV-C/$TiO_2$ achieved the best techno-economic and energy performance.
- UV-C minimizes the total cost: 10 € $m^{-3}$ for MTLC and 1 € $m^{-3}$ for DXMT.

## GRAPHICAL ABSTRACT

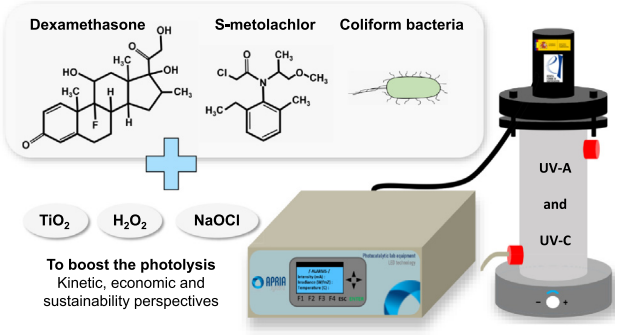


## ARTICLE INFO

Editor: Damià Barceló

*Keywords:*
CEC
Disinfection
UV-C
Photolysis
LED
AOP

## ABSTRACT

Disinfection commonly follows conventional treatments in wastewater treatment and remediation plants aiming at reducing the presence of pathogens. However, the presence of the so called "micropollutants" has emerged as a serious concern, therefore developing tertiary treatments that are not only able to remove pathogens but also to degrade micropollutants is worth investigating. Nowadays, UV-C photo-degradation processes are widely used for disinfection due to their simplicity and easy operation; additionally, they have shown potential for the removal of contaminants of emerging concern. Conventional mercury lamps are being replaced by light-emitting diodes (LEDs) that avoid the use of toxic mercury and can be switched on and off with no effect on the lamp lifetime. This work aims to comparatively evaluate the performance of several photo-degradation technologies for the removal of two targeted micropollutants, the pharmaceutical dexamethasone (DXMT) and the herbicide S-metolachlor (MTLC), using UV irradiation doses typical of disinfection processes. To this end, the technical performance of UV-A/UV-C photolysis, UV-A/UV-C photocatalysis, UV-C/$H_2O_2$ and UV-C/NaOCl has been compared. The influence of operating conditions such as the initial concentration of the pollutants (3 mg $L^{-1}$ - 30 mg $L^{-1}$, concentrations found in membrane or adsorption remediation steps), pH (3 − 10), and water matrix (WWTP secondary effluent, and ultrapure water) on the degradation efficiency has been studied. The economic evaluation in terms of electricity and chemicals consumption and the carbon footprint has been evaluated. UV-C photolysis and UV-C photocatalysis appear as the most suitable technologies for the degradation of DXMT and MTLC, respectively, in terms of kinetics ($1.53{\cdot}10^{-1}$ $min^{-1}$ for DXMT and $1.96{\cdot}10^{-2}$ $min^{-1}$ for MTLC), economic evaluation (1 € $m^{-3}$ for DXMT and 32 € $m^{-3}$ for MTLC) and environmental indicators (0.5 g-$CO_2$ for DXMT and 223.1 g-$CO_2$ for MTLC).

## 1. Introduction

In the last decades, UV-C based processes have been widely used, mostly for disinfection, with low or medium pressure mercury lamps as the most frequently used light source. Despite this technology is widely known, it

* Corresponding author.
*E-mail address:* ortizi@unican.es (I. Ortiz).

http://dx.doi.org/10.1016/j.scitotenv.2022.161376
Received 27 October 2022; Received in revised form 16 December 2022; Accepted 31 December 2022
Available online 6 January 2023

entails economic and environmental problems, such as frequent lamp replacement, low efficiency, toxicity of mercury, and lifetime that is shortened with each lamp operating cycle (Čizmić et al., 2019). For this reason, light emitting diodes (LEDs) have arisen to overcome the mentioned problems. Commercial availability of LEDs has considerably increased in recent years, promoting their widespread use (Ferreira et al., 2020; Dominguez et al., 2016; Ou et al., 2016). Moreover, they present additional benefits, such as higher stability, that is switch on and off cycled do not affect LEDs lifetime, and the ability to emit the whole light at a specific wavelength. These characteristics make them suitable for disinfection (Hansen et al., 2021; Office of Energy Efficiency and Renewable Energy, 2022).

Pathogens pose a risk to humans and ecosystems, so regulations across the world consider that their monitoring is mandatory for the reuse of wastewaters, aiming at reducing their propagation. In particular, the Royal Decree 1620/2007 of the Spanish legislation, establishes the legal regime for the reuse of treated water, in which *Escherichia coli* (*E. coli*) bacteria are regulated. Some authors have investigated the disinfection of microorganisms under different wavelengths; for instance, Lui et al. (2016) used 12 different wavelengths from 270 to 740 nm, achieving the fastest inactivation of *E. coli* at 270 nm. Despite UV-C LED disinfection being an effective technology, it is less efficient than conventional light sources, so most commonly these lamps have been used in combination with mercury lamps, working at different wavelengths or with additional treatments to achieve faster inactivation (Choi et al., 2020; Hansen et al., 2021; Malvestiti and Dantas, 2019; Matafonova and Batoev, 2022; Szeto et al., 2020). Although these alternatives achieve faster removal of microorganisms, economic and sustainable issues must be considered in the selection of the final treatment.

UV-C LED photolysis has been also proposed as a promising approach for degradation of contaminants of emerging concern (CECs) in aqueous solution. Photolysis is based on the use of light as energy source: when photons are absorbed by molecules, both physical and chemical changes take place in the target compounds, leading to their transformation to intermediate products or further decomposition to mineral end-products (Klavarioti et al., 2009; Olatunde et al., 2020). Most organic molecules show UV–Vis absorption bands at relatively low UV wavelengths, such as UV-C (Choi et al., 2020; Olatunde et al., 2020), making UV-C photodegradation technology ideal for remediation of polluted waters. The efficiency of the degradation is greatly influenced by the absorptivity of the pollutant, the properties of the light source, such as wavelength and intensity, and the molecule structure.

Several studies have reported the presence of different pharmaceuticals in wastewaters, such as antibiotics, anti-inflammatories, antidepressants, analgesics, and natural and synthetic hormones (Bradley et al., 2020; Costa et al., 2021; Diamanti et al., 2020; Escudero et al., 2021; Köck-Schulmeyer et al., 2021; Liu et al., 2020a; Pariente et al., 2022; Parra-Saldivar et al., 2021; Serra-Compte et al., 2021; Solaun et al., 2021). Due to COVID-19 pandemic, the glucocorticoid pharmaceutical dexamethasone (DXMT) has been widely used in the treatment of the symptoms in Intensive Care Units (ICUs), so it can be found in wastewaters, together with many other pharmaceuticals. Furthermore, some authors investigated the application UV-C photolysis for dexamethasone degradation mostly using conventional mercury lamps at 254 nm. Some authors, such as Markic et al. (2018) investigated the DXMT removal, using $H_2O_2$ and $S_2O_8^{2-}$ to enhance the degradation provided by UV-C photolysis, but they did not take into account the environmental and economic issues, such as the increment in the total operation cost due to the addition of chemicals and the low efficiency of the mercury lamp. Ou et al. (2016) explored the degradation of ciprofloxacin, with similar chemical structure to DXMT, using UV LEDs at different wavelengths and achieving the highest removal efficiency at 280 nm, which opens the possibility of using different UV-C wavelengths other than 254 nm. Phytosanitary compounds are also of interest because of their widespread use and recalcitrant behavior; they also can be found in natural waters (Bradley et al., 2020; Diamanti et al., 2020; Hildebrandt et al., 2007, 2008; Köck-Schulmeyer et al., 2021; Liu et al., 2020b; Solaun et al., 2021). In particular, S-metolachlor (MTLC), a chloroacetamide herbicide, is widely used to control weeds' growth, and it is slowly biodegraded (Wu et al., 2007). Some authors reported the UV degradation process of MTLC and most of the studies used oxidants or different treatments to enhance the removal kinetics. For instance, Collivignarelli and Sorlini (2004) used ozone combined with UV-C; nevertheless, the operational cost that represents the energy and the addition of chemicals in those processes has not been evaluated so far.

Even though UV-C photolysis is a promising technology to remove pathogens and CECs, this double objective is still a novel approach, as the most extended alternative consists on the use of mercury lamps or combined treatments such as photocatalysis and UV/$H_2O_2$ (Choi et al., 2020; Rathnayake et al., 2020; Sánchez-Montes et al., 2020). However, in some cases, UV-C photolysis is not able to remove some persistent compounds or to achieve their total mineralization. Therefore, Advanced Oxidation Processes (AOPs) have been also investigated, because they are efficient for the degradation of recalcitrant compounds present in aqueous media (Chaves et al., 2020; Escudero et al., 2017). Some of them make use of oxidants to produce radical species, such as hydroxyl radicals. For instance, heterogeneous photocatalysis with $TiO_2$, UV/$H_2O_2$ and UV/NaOCl have been reported as effective AOPs for remediation of wastewater containing contaminants of emerging concern (Hurwitz et al., 2014; Neghi and Kumar, 2017; Stankov et al., 2021). AOPs have been widely evaluated from a technical point of view, understanding the kinetics of the degradation of different compounds and their degradation route. Nevertheless, although AOPs could enhance the kinetics of photolysis, they could lead to inefficient and non-sustainable systems, in terms of economics and environment, due to the use of expensive reagents and high energy consumption (Choi et al., 2020). Therefore, here we report the technical performance of UV light technologies, together with an environmental and techno-economical evaluation to facilitate the decision-making process ending with selection of the most adequate alternative.

## 2. Methodology

### 2.1. Materials

Dexamethasone (>98 %, HPLC) and metolachlor PESTANAL© were purchased from Sigma-Aldrich (USA). Their CAS number, formula, chemical structure and other properties are summarized in Table S.1. Chromatographic-grade solvent acetonitrile was acquired from LiChrosolv® and used as received (gradient grade for liquid chromatography). Hydrochloric acid (HCl, 0.1 M, Fisher Scientific, U.K.) and sodium hydroxide (NaOH, 50 %, Merck KGaA, Germany) were used to control the pH of the solution. In order to increase the degradation rate of the target compounds, the formation of hydroxyl radicals (OH·) and free chlorine was promoted by the photolysis of hydrogen peroxide ($H_2O_2$) and sodium hypochlorite (NaOCl) by UV radiation, or the excitation of titanium dioxide ($TiO_2$) photocatalyst. For the UV/$H_2O_2$ experiments, hydrogen peroxide ($H_2O_2$, 30 %) was purchased from PanReac (Germany), also sodium hydrogen bisulfite ($NaHSO_3$, 40 %, PanReac, Germany) was used to remove the excess of hydrogen peroxide to measure the degradation of the target compound. For the UV/NaOCl experiments, sodium hypochlorite (NaOCl, 10 %) was acquired from Labkem (Spain). The photocatalytic experiments were performed using 0.5 g $L^{-1}$ of $TiO_2$ Aeroxide P-25 photocatalyst (Evonik, Germany). Wastewater samples were collected from the secondary effluent of Vuelta Ostrera Wastewater Treatment Plant (WWTP) (Cantabria, Spain) and stored in amber bottles in the dark at 4 °C. The WWTP effluent characteristics are detailed in Table S.2.

### 2.2. Experimental design

To perform the photo-degradation experiments, a lab-scale photoreactor (Apria Systems S.L., Spain) was used working in batch mode (Fig. 1a). It was a cylindrical borosilicate glass sheathed photo-reactor with a silver finish to maximize the LEDs effect. It has a capacity of 500 mL and is provided with two outlets to allow samples collection in

continuous operation. The UV LED lamp was placed in the center of the reactor, fixed at 1.2 cm distance from the reactor walls (Fig. 1b). The UV-C LED lamp has the maximum peak of emission at 278 nm, 12 W $m^{-2}$ of maximum irradiance and 14 W of maximum power, and the UV-A LED lamp emitted at 365 nm with 1500 W $m^{-2}$ of maximum irradiance and 53.2 W of maximum power consumption. They both are provided with 20 LEDs, a ventilation system, a temperature probe and magnetic stirrer. The reactor is connected to a control panel that allows modifying LEDs radiation, and reading the intensity (mA), irradiance (W $m^{-2}$) and temperature (°C).

Aliquots were taken out of the reactor in each experiment to measure the concentration of CECs in a high-performance liquid chromatograph (HPLC). All experiments were performed in duplicate, and the average values are reported. Moreover, every graph has error bars representing the average error of duplicate measurements.

### 2.3. Analytical methods

The high-performance liquid chromatograph (HPLC; Agilent, 1100 series) was used with a Zorbax extend-C18 column (3.0 × 150 mm, 5 μm) and a diode array detector (DAD). The excitation wavelength of the spectrophotometer was adjusted to 240 nm for DXMT and 214 nm for MTLC. The inlet flow rate was 0.5 mL $min^{-1}$ in DXMT case and 0.7 in MTLC. A mixture of acetonitrile and ultrapure water with a 40/60 ratio was used as mobile phase for DXMT and with a ratio 60/40 for MTLC, and the injection volume was 50 μL for both. The retention time for DXMT was 3 min, while for MTLC was 4.5 min, and the total time for both runs was 6 min. The detection limit for DXMT was 0.05 mg $L^{-1}$, and 0.1 mg $L^{-1}$ for MTLC. The degradation removal of total coliform and *E. coli* bacteria after the UV-C LED treatment was evaluated. The method followed was Colilert-18 (IDEXX, Spain), based on the ISO 9302-2: Water quality – enumeration of *Escherichia coli* and coliform bacteria. The samples collected in the experiments were mixed with Colilert-18 reactant poured in a tray and sealed. Incubation for 18 h at 37 °C was carried out before quantification. The water samples were taken from the secondary effluent of Vuelta Ostrera wastewater treatment plant, in Cantabria (Spain). In the UV/$H_2O_2$ and UV/NaOCl experiments, the concentration of the target compound was also measured in HPLC-DAD. However, the remaining oxidant concentration in UV/$H_2O_2$ was measured using specific tests (purchased from Merk KGaA, Germany), which can measure from 0 to 1000 mg $L^{-1}$ of $H_2O_2$, and the remaining $H_2O_2$ concentration was quenched with sodium hydrogen bisulfite ($NaHSO_3$, 40 %, PanReac, Germany). For the UV/NaOCl, the total and free chlorine were monitored with two digital colorimeters, Checker Total Chlorine HI 711 and Checker Free Chlorine HI 701 (both from HANNA Instruments, Romania), that are able to measure from 0 to 3.5 mg $L^{-1}$ of total chlorine and from 0 to 2.5 mg $L^{-1}$ of free chlorine, using DPD (N,N-diethyl-*p*-phenylenediamine) Total and Free Chlorine Permachem Reagents (HACH, Germany). Within the UV-A/$TiO_2$ and UV-C/$TiO_2$ experiments, the titanium dioxide powder was dispersed in the water matrix and the samples were filtered through a nylon syringe filter (0.45 μm, FILTERLAB®) to remove the particles of $TiO_2$. The irradiance of the UV-A and UV-C LEDs was measured with a photo-radiometer HD 2102.1 from Delta OHM (Italy), with UV-A and UV-C probes. The mineralization was measured in a total organic carbon analyzer TOC-V CPH with auto-sampler ASI-V (Shimadzu, Japan). The hydroxyl radical quantification was performed following the methodology described by Tai et al. (2004).

## 3. Results and discussion

### 3.1. Influence of the water matrix and operating parameters in photolysis

Secondary effluents from WWTPs may contain different micropollutants but also different types of microorganisms, such as bacteria or viruses. Among bacteria, the effectiveness of UV-C LED in the removal of *E. coli* has been considered. The degradation of the contaminants of emerging concern was carried out with 30 mg $L^{-1}$ of initial concentration of the target compounds (DXMT and MTLC) and 3 W $m^{-2}$ of UV-C irradiance. Disinfection experiments were performed starting with 50,000 CFU per 100 mL of *E coli*, and 3 W $m^{-2}$ of UV-C irradiance. Fig. 2 shows representative degradation kinetic curves of emerging contaminants and bacteria.

As observed in Fig. 2, under the conditions of this work, *E. coli* bacteria were removed with a UV-C radiation dose of 90 mJ $cm^{-2}$, achieving >4-log reduction. The difference in the kinetics of the degradation of DXMT and MTLC, was attributed to the difference in the absorption of UV-C light at 278 nm that gave 90 % degradation of DXMT for 540 mJ $cm^{-2}$ and 90 % elimination of MTLC for 10,800 mJ $cm^{-2}$. Fitting the data of Fig. 2 to first-order kinetic equations, the kinetic parameters obtained were $4.35{\cdot}10^{-2}$ $min^{-1}$ for DXMT, $3.60{\cdot}10^{-3}$ $min^{-1}$ for MTLC and $9.12{\cdot}10^{-1}$ $min^{-1}$ for *E coli*. As can be observed in Fig. 2 and in the kinetic data, the kinetic constant of the removal of *E. coli* is much higher than that of DXMT and MTLC. Therefore, this study has evaluated the comparative performance of different photodegradation technologies aimed at the removal of micropollutants using similar UV doses to those required for disinfection.

The photo-degradation of the target contaminants of emerging concern, MTLC and DXMT, was investigated for various initial concentrations, in the range between 3 mg $L^{-1}$ to 30 mg $L^{-1}$, and in different water matrices: ultrapure water (UPW) and wastewater effluent (WW). The concentrations of the target pollutants represent values that can be found after the application of different water remediation processes, e.g., membrane filtration, solid adsorption, etc. Worth mentioning is the work of Cantalupi et al. (2020) who did not find any significant influence of DXMT concentration in the range of concentration between 10 mg $L^{-1}$ and 50 μg $L^{-1}$, achieving

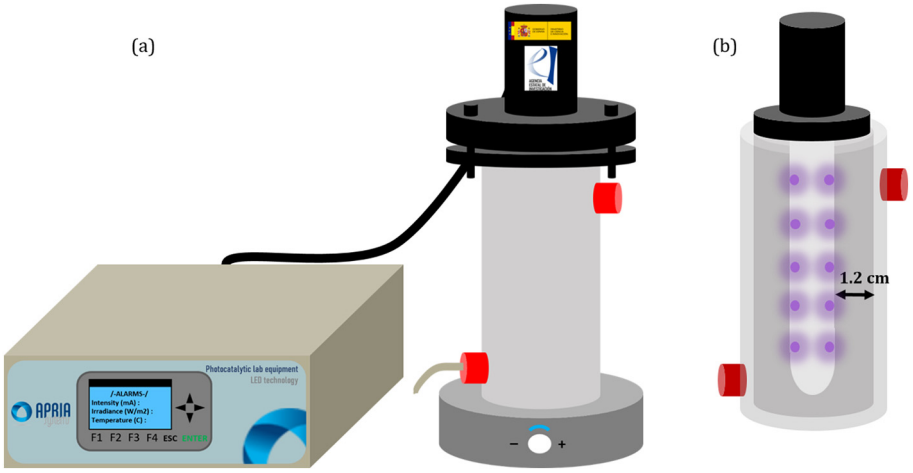


**Fig. 1.** (a) UV-C LED photo-reactor and control panel, (b) UV-C LED lamp inside the photo-reactor.

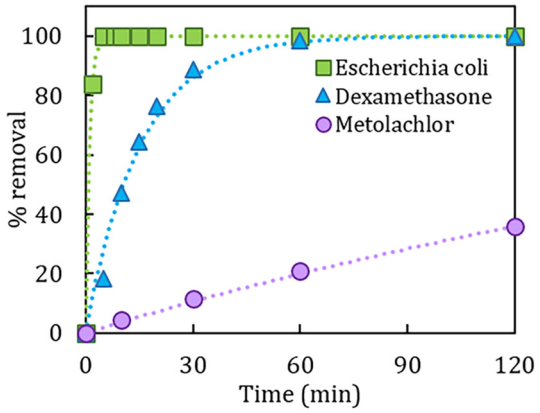


**Fig. 2.** Removal kinetics of *E. coli* bacteria, DXMT and MTLC with UV-C photolysis in WWTP secondary effluent: UV-C irradiance = 3 W $m^{-2}$, [*E. coli*]$_0$ = 50,000 CFU per 100 mL, [DXMT]$_0$ = [MTLC]$_0$ = 30 mg $L^{-1}$, pH natural = 6, reaction volume = 0.45 L. Dashed lines represent the simulated pseudo-first order kinetics.

degradation constants of $1.39{\cdot}10^{-2}$ $min^{-1}$ and $1.17{\cdot}10^{-2}$ $min^{-1}$, respectively, after applying UV-C photolysis in tap water.

Fig. 3 depicts the experimental results of the degradation of MTLC and DXMT for an irradiance of 12 W $m^{-2}$ and 1.2 W $m^{-2}$, respectively. Different irradiances were used for both contaminants because of the different degradation rates.

The experimental data shown in Fig. 3 were fitted to a pseudo-first kinetic model, according to Eq. (1), obtaining the fitting parameters collected in Table S.3.

$$\frac{dC}{dt} = -k_{app} \cdot C \rightarrow \ln(C_0) - \ln(C) = -k_{app} \cdot t \quad (1)$$

where $C_0$ is the initial concentration of the contaminant (mg $L^{-1}$), C is the concentration at time t (mg $L^{-1}$), $k_{app}$ is the apparent first-order kinetic constant, and t the reaction time.

Moreover, it is possible to calculate the required dose for a fixed degradation percentage, according to Eq. (2).

$$\text{Dose}\left(\text{mJ cm}^{-2}\right) = \frac{\text{Irradiance}\left(\text{W m}^{-2}\right) \cdot \text{time (s)}}{10} \quad (2)$$

The degradation kinetic constant of DXMT increases while decreasing the initial concentration (Fig. 3b and Table S.3). A similar trend has been previously observed for other contaminants in the same range of initial concentrations (Cantalupi et al., 2020; Rasolevandi et al., 2019; Solís et al., 2021), even though no influence was observed for concentrations between 10 mg $L^{-1}$ and 50 μg $L^{-1}$ (Cantalupi et al., 2020). The DXMT molecule is highly susceptible to degradation by UV-C photolysis and thus, the higher the concentration of contaminant the higher the concentration of oxidation products that may be present in the aqueous solution and the competition for incident photons increases (Silva et al., 2014). For the degradation of MTLC, it was not observed influence of the initial concentration on the degradation rate, in the studied range of initial concentrations (Fig. 3a and Table S.3). A similar performance was previously reported for molecules with similar structure. Ferhi et al. (2021) investigated the photodegradation of atrazine with UV-C photolysis at 254 nm, whose maximum absorption wavelength is 225 nm, at different concentrations (from 0.5 to 10 μg $L^{-1}$) in groundwater and wastewater, and they did not observe any influence on the initial concentration.

The influence of the water matrix was tested with ultrapure water and with the secondary effluent of a wastewater treatment plant, both spiked with the target contaminants (Fig. 3 and Table S.3). Due to the small differences in the apparent rate constants, the influence of the water matrix is considered negligible for both contaminants. Moreover, a specific contribution of wastewater constituents, such as the interference of salts and natural organic matter, in the photodegradation rate can be excluded. Raschitor et al. (2021) studied the influence of the water matrix in the degradation of three insecticides, imidacloprid, clothianidin and thiamethoxam in distilled and surface water and they did not observe any effect on the photolytic removal using UV-C at 254 nm. Farkas et al. (2018) analyzed the influence of inorganic salts, such as $HCO_3^-$, $Cl^-$, $SO_4^{2-}$ or $NH_4^+$, in the photolytic degradation of two herbicides, monuron and diuron, with UV-C at 254 nm in ultrapure, natural, river and thermal waters; and the authors did not report any significant effect of the water matrix. On the contrary, Dimou et al. (2005) determined the influence of different water matrices (sea, river, lake, and distilled water) and some parameters such as dissolved organic matter and nitrate ions under solar and simulated solar irradiation, reporting that the dissolved organic matter inhibits the photolytic reaction, whereas it is promoted in the presence of nitrate ions. Moreover, Cantalupi et al. (2020) and Marson et al. (2021) revealed the possibility of the competition of some compounds for the UV-C light, such as natural organic matter (NOM), that absorbs UV-C light, leading to a reduction in the available light for the degradation of the target compound, because they compete for a fraction of light. Other operating parameters might have influence on the degradation, such as the water conductivity and turbidity. The wastewater effluent used in this study had low values of conductivity, turbidity, nitrates, and chemical oxygen demand (COD). It was observed that these parameters do not exert influence on the degradation rate of the contaminants.

The effect of pH on the photolysis of 30 mg $L^{-1}$ of DXMT and MTLC was assessed for different irradiances (3 W $m^{-2}$ for DXMT and 12 W $m^{-2}$ for MTLC) because of their different degradation rates, and pH values between

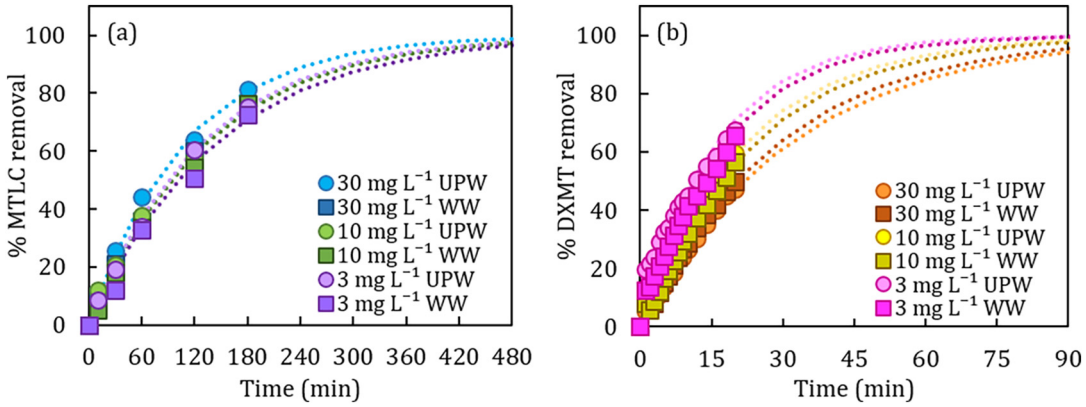


**Fig. 3.** MTLC (a) and DXMT (b) removal data for the experiments at different initial concentration, with UV-C photolysis in ultra-pure water (UPW) and wastewater effluent (WW). UV-C irradiance = 12 W $m^{-2}$ (for MTLC), 1.2 W $m^{-2}$ (for DXMT), pH natural = 6, reaction volume = 0.45 L. Dashed lines represent the simulated pseudo-first order kinetics.

3 and 10. Based on the results collected in Fig. S.1, it was confirmed that changing the pH in the range 3.0 < pH < 10.0 has no significant effect on UV-C photolysis of both target compounds, because MTLC has no $pK_a$ value and DXMT has a $pK_a$ of 12.42 (Drugbank, 2022), out of the working range and thus, the molecules did not dissociate at the studied conditions. Similar results were reported by Khan et al. (2017) at pH values of 3, 5.7 and 10 with desethyl-atrazine and desisopropyl-atrazine which possess similar molecular structure to MTLC. This was also reported by Rasolevandi et al. (2019) for DXMT. Moreover, a decrease of the pH during the experiment was noticed, but it was attributed to the formation of organic acids (Guelfi et al., 2018; Rancaño et al., 2021; Sakkas et al., 2004).

Considering the grounds of photolysis, when light passes through a molecule, its energy is used to move an electron from a bonding or non-bonding orbital to empty anti-bonding orbitals. This means that the target molecule must have π bonds or atoms with non-bonding orbitals, that is, double or triple bond, or an atom with lone pair of electrons (nitrogen, oxygen, or halogen) to absorb UV light higher than 200 nm (Reusch and Clark, 2020). For instance, the energy to break short chain molecules with only two carbon atoms, even though some have π bonds and lone pairs, is higher than the UV-C energy, so they cannot be broken only with UV-C light. Worth to mention is that the maximum absorption wavelength increases with electron delocalization. The bond breakage energy of some organic compounds has been collected in literature, depending on the ultraviolet wavelength range (Liang et al., 2010; Masschelein, 2002).

In the case of DXMT, the double bond carbon-oxygen, the simple bond carbon-fluorine, the simple bond between a benzene ring and a hydroxyl group, and the polycyclic aromatic hydrocarbons (PAHs) will be broken in the working conditions. Cantalupi et al. (2020), Ou et al. (2016), and Rasolevandi et al. (2019) also reported that the first phase in the degradation of DXMT, ciprofloxacin and similar molecular structures by direct 280 nm UV-C photolysis is the cleavage of its aromatic C—F bonds. Besides, 40 % of fluoride in solution is eliminated during 480 min of experiment, thus supporting the mechanism. In addition, some studies in the literature identified the intermediate products of its degradation. For instance, prednisolone was found as a direct intermediate of DXMT, that is formed when the parent compound loses the fluorine heteroatom and, also acetic acid, formaldehyde, hexane-1,6-diol, 1-((hydroxymethyl)thio)ethanol, and (*E*)-but-2-ene-1,2,4-triol were found during the UV-C/Iodide treatment of DXMT (Rasolevandi et al., 2019). On the other hand, Quaresma et al. (2021) analyzed the intermediate products of the reaction pathway in different AOPs. For UV-C photolysis, they observed that the DXMT molecule loses one OH group whereas the DXMT degradation by UV-C/$TiO_2$ loses the F heteroatom, and OH groups.

Besides, the MTLC molecule can only be broken at the double bond carbon-oxygen and carbon-chlorine bond, followed by a homolytic or heterolytic cleavage. Moreover, the breakage of aromatic acids by UV-C may result in decarboxylation, deamination or ring breakage (Kalisvaart, 2001). Wu et al. (2007) studied the photodegradation process of MTLC under UV-C at 254 nm irradiation, in which dechlorination, hydroxylation, oxoquinolone formation, and demethylation reactions were observed during the photolysis process and the intermediate products were analyzed. Likewise, Souissi et al. (2013) evaluated the intermediates formed during UV photolysis with a lamp emitting from 200 to 1100 nm. They observed dechlorination, hydroxylation, cyclization and demethylation reactions, as well. Some authors detailed the photolytic degradation of phytosanitary compounds with similar molecules as MTLC under UV-C irradiation, showing that the C—Cl bond could be broken under UV-C photolysis because of its length and low polarity (Fan et al., 2022; Khan et al., 2017; Mermana et al., 2017; Sakkas et al., 2004; Silva et al., 2014).

Regarding coliform bacteria, UV absorption by DNA is due to the absorption by the nucleotide bases. In the case of *E. coli*, the DNA containing the genetic material of the cellular organisms absorbs UV-C irradiation at 278 nm, and thus it can be damaged. The absorption by DNA at that UV range is due to the absorption of the nucleotide bases: adenine, guanine, cytosine, and thymine, in which carbon-oxygen double bonds will be broken, and excision of PAHs will take place. Moreover, UV-C can damage the intracellular chromophores. This mechanism has been already proposed in literature. Kalisvaart (2001), and Kalisvaart (2004) found that the most common products from the nucleotide damage by UV-C irradiation are thymine dimers, in which two thymine molecules joint covalently by cyclobutene. This also confirms the high degradation rate of coliform bacteria by UV-C light.

Therefore, these results confirm the high dependence of the different bonds present in the organic molecules on the light absorbance, and thus, it explains the different degradation kinetics. Moreover, the comparison with the results previously reported in the literature at different wavelengths and technologies confirms the suggested bond breakage mechanism.

### 3.2. UV light driven AOPs

The degradation kinetics by UV-C photolysis could be improved by the use of advanced oxidation processes (AOPs), reducing the reaction time and costs. Therefore, the photo-degradation of metolachlor and dexamethasone was also tested under various UV light driven AOPs, such as heterogeneous photocatalysis (with UV-A and UV-C), UV-C/$H_2O_2$, and UV-C/NaOCl, to achieve total degradation of the target CECs with faster kinetic rates.

Photocatalysis is a well-known technology for the treatment of polluted waters with persistent compounds, based on the formation of hydroxyl radicals and other oxidant species during the photoexcitation of the $TiO_2$ semiconductor. A simplified photocatalysis mechanism is presented in Eqs. (3) and (4) (Barquín et al., 2022; Nosaka and Nosaka, 2017; Ribao et al., 2019).

$$TiO_2 + hv \rightarrow e^- + h^+ \quad (3)$$

$$h^+ + H_2O \rightarrow H^+ + \cdot OH \quad (4)$$

Photocatalytic experiments were conducted with 30 mg $L^{-1}$ of the target compound (MTLC or DXMT) and 0.5 g $L^{-1}$ of $TiO_2$ (catalyst concentration based on previous results) (Barquín et al., 2022), in ultrapure water and natural pH. Fig. 4 depicts the experimental results of the degradation of MTLC and DXMT, with an irradiance of 12 W $m^{-2}$ in UV-C and 1500 W $m^{-2}$ in UV-A, both at the 100 % of the lamp power, as it was not possible to work with the same irradiance. In every photocatalytic experiment, the water medium was contacted 30 min in the dark to test the possible adsorption of the contaminants in the catalyst.

The MTLC degradation was highly improved with the addition of $TiO_2$ compared to photolytic processes. The MTLC degradation by photolysis with UV-A was negligible while with $TiO_2$ achieved >90 % of degradation in 10 min. In the UV-C case, the difference was lower, but photocatalysis also improved the degradation of MTLC (Fig. 4a and Table S.4). This trend can be explained due to the role of the hydroxyl radicals generated with the considered four technologies, as shown in Fig. S.3. UV-A/$TiO_2$ was the process that generated more OH· radicals, although their formation rate followed two different slopes: the first part, until 10 min, showed the highest slope that afterwards slowed down. This behavior was also observed in the degradation kinetics of both contaminants with UV-A/$TiO_2$, supporting the influence of hydroxyl radicals in the photo-degradation rate. Regarding UV-C/$TiO_2$, the degradation of DXMT and MTLC proceeded at a constant rate in the same way that the generation of ·OH radicals. Then, the generation of hydroxyl radicals in UV-A and UV-C photolysis was less significant.

The DXMT degradation by UV-A was highly improved with photocatalysis, because of the action of OH· radicals. Nevertheless, UV-C photocatalysis performed worse than photolytic degradation (Fig. 4b and Table S.4). This behavior can be explained by the susceptibility of DXMT molecules to be degraded by UV-C, which is hindered by the turbidity generated by the catalyst addition (higher than 1000 NTU). For a comprehensive comparison, the main parameters and results of photocatalysis and photolysis with UV-A and UV-C, such as lamp irradiance, energy consumption and degradation rate constants ($k_{app}$) are also summarized in Table S.4.

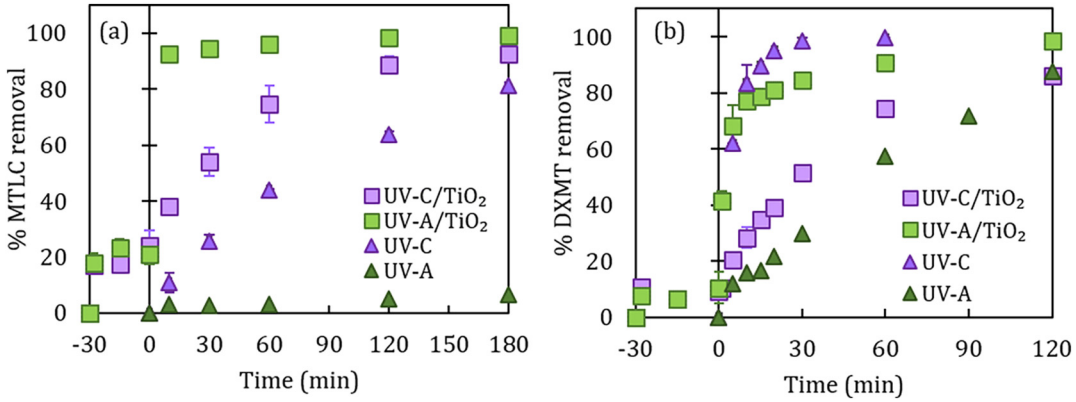


**Fig. 4.** Metolachlor (a) and dexamethasone (b) removal in photocatalysis with UV-C, photocatalysis with UV-A, photolysis with UV-C and photolysis with UV-A experiments. $[DXMT]_0 = [MTLC]_0 = 30$ mg $L^{-1}$, $[TiO_2]_0 = 0.5$ g $L^{-1}$, UV-C irradiance = 12 W $m^{-2}$, UV-A irradiance = 1500 W $m^{-2}$, ultrapure water, pH natural = 6, reaction volume = 0.45 L.

Therefore, the obtained results show that, from a kinetic perspective, photocatalysis with UV-A is the fastest treatment for both contaminants in the present working conditions. Moreover, UV-C photolysis is the most efficient process for the breakage of molecules with bonds absorbing in the UV-C such as DXMT, whereas more recalcitrant molecules such as MTLC require indirect oxidation mediated by hydroxyl radicals.

The UV-C/$H_2O_2$ process was also tested as an alternative AOP to enhance the photolysis of MTLC and DXMT. UV irradiation with wavelength (λ) <280 nm induces the photolytic rupture of the hydrogen peroxide molecule to form hydroxyl radicals (Eq. (5)). However, the overdose would lead to the reaction with OH• radicals and formation of $HO_2$· radicals, less reactive (Eq. (6)) (Cerreta et al., 2019; Markic et al., 2018). Moreover, the molecular extinction coefficient of $H_2O_2$ increases decreasing the wavelength.

$$H_2O_2 + hv \rightarrow 2\ HO\cdot \quad (5)$$

$$H_2O_2 + HO\cdot \rightarrow HO_2\cdot + H_2O \quad (6)$$

To assess the influence of the hydrogen peroxide concentration, it was changed in a range from 30 mg $L^{-1}$ to 3000 mg $L^{-1}$. Every UV-C/$H_2O_2$ experiment was carried out with an initial concentration of 30 mg $L^{-1}$ of the target contaminant, in ultrapure water, at natural pH and 12 W $m^{-2}$ of irradiance. Fig. S.2 shows the results of UV-C/$H_2O_2$ experiments for the degradation of DXMT compared to those of UV-C photolysis. These experiments were performed with 30 mg $L^{-1}$, 100 mg $L^{-1}$, 300 mg $L^{-1}$, 700 mg $L^{-1}$, 1500 mg $L^{-1}$, and 3000 mg $L^{-1}$ of $H_2O_2$, corresponding to molar ratios of [$H_2O_2$]:[DXMT], 12:1, 39:1, 116:1, 271:1, 580:1, and 1160:1. The DXMT molecule is highly susceptible to degradation by UV-C photolysis, and even though UV-C/$H_2O_2$ technology achieves the higher hydroxyl radical generation (Fig. S.3), those radicals formed by hydrogen peroxide photolysis are unable to increase the degradation rate (Fig. S.2). Table S.4 details the kinetic results of DXMT degradation with 300 mg $L^{-1}$ of $H_2O_2$. Markic et al. (2018) achieved 20 % increase in the degradation of DXMT working at 254 nm, because the photolytic breakage of the hydrogen peroxide molecule was favored at lower wavelengths, and thus, more OH· radicals were formed to attack the DXMT molecule. However, they detected a similar trend regarding the different oxidant concentrations, with no improvement in the degradation kinetics.

Fig. 5a shows the results of the UV-C/$H_2O_2$ experiments for the degradation of MTLC compared to those of UV-C photolysis, while Fig. 5b shows the removal of hydrogen peroxide during the experiments. These experiments were performed with 30 mg $L^{-1}$, 100 mg $L^{-1}$, 200 mg $L^{-1}$, 700 mg $L^{-1}$, and 1000 mg $L^{-1}$ of $H_2O_2$, corresponding to molar ratios of [$H_2O_2$]:[MTLC], 8:1, 28:1, 55:1, 200:1, and 285:1. The kinetic results of MTLC degradation with the $H_2O_2$ concentration of 200 mg $L^{-1}$ is detailed in Table S.4, and the initial concentrations of hydrogen peroxide and all the kinetic results are summarized in Table S.5.

The MTLC molecule is more recalcitrant and less susceptible to degradation by UV-C photolysis, so it requires indirect oxidation by hydroxyl radicals; the use of the hydrogen peroxide reinforces the generation of hydroxyl radicals and contributes to improve the degradation kinetics (Fig. 5a), as previously observed by other authors (Sánchez-Montes et al., 2020; Wu et al., 2007). The degradation rate of MTLC increased while increasing the $H_2O_2$ concentration, due to the continuous presence of $H_2O_2$ in solution during the experiments (Fig. 5b) and the more prominent formation of hydroxyl radicals with this technology (Fig. S.3). Nevertheless, with concentrations higher than 200 mg $L^{-1}$ of $H_2O_2$, the formation of $HO_2$· radicals decreases the process efficiency, also observed by Wu et al. (2007).

Therefore, the UV-C/$H_2O_2$ process increases the efficiency of the treatment of persistent organic pollutants, such as MTLC. For these working conditions, the recommended $H_2O_2$ concentration for MTLC removal would be 200 mg $L^{-1}$, while $H_2O_2$ does not improve the degradation kinetics of DXMT (Fig. S.2). Another key aspect is the consumption of $H_2O_2$ during the experiments, since hydrogen peroxide is toxic and its discharge is not allowed, which makes necessary a neutralization stage; besides, using excess of $H_2O_2$, supposes an unnecessary increment of costs and therefore, future studies will consider the continuous addition of $H_2O_2$. In the degradation runs of MTLC, even though the amount of hydrogen peroxide has been optimized, >70 % remains in solution after 120 min (Fig. 5b), which assures the presence of hydroxyl radicals, but demands further post-treatment.

The UV-C/NaOCl process was analyzed to enhance the photolysis of MTLC and DXMT as well. This technology uses UV-C to break NaOCl and form reactive species, such as HOCl (Eqs. (7), (8), and (9)) (Cerreta et al., 2019). NaOCl is used because of its higher UV absorbance compared to hydrogen peroxide and it produces three reactive species (Ngumba et al., 2020). Additionally, NaOCl dissociates in different radical species depending on the pH of the medium (including hydroxyl, chlorine and oxygen radicals). At natural pH of the MTLC or DXMT solution (5.5), the predominant specie is HOCl (which is the most reactive specie), and when the pH increases, $OCl^-$ is formed.

$$NaOCl + H_2O \rightarrow HOCl + NaOH^- \quad (7)$$

$$HOCl + hv \rightarrow HO\cdot + \cdot Cl \quad (8)$$

$$OCl^- + hv \rightarrow \cdot O^- + \cdot Cl \quad (9)$$

UV-C/NaOCl experiments were carried out with 30 mg $L^{-1}$ of the target contaminant, in ultrapure water, at natural pH and 12 W $m^{-2}$ of irradiance. Moreover, to evaluate the influence of the sodium hypochlorite concentration, it was changed from 10 mg $L^{-1}$ to 100 mg $L^{-1}$. Fig. 6 shows the UV-C/

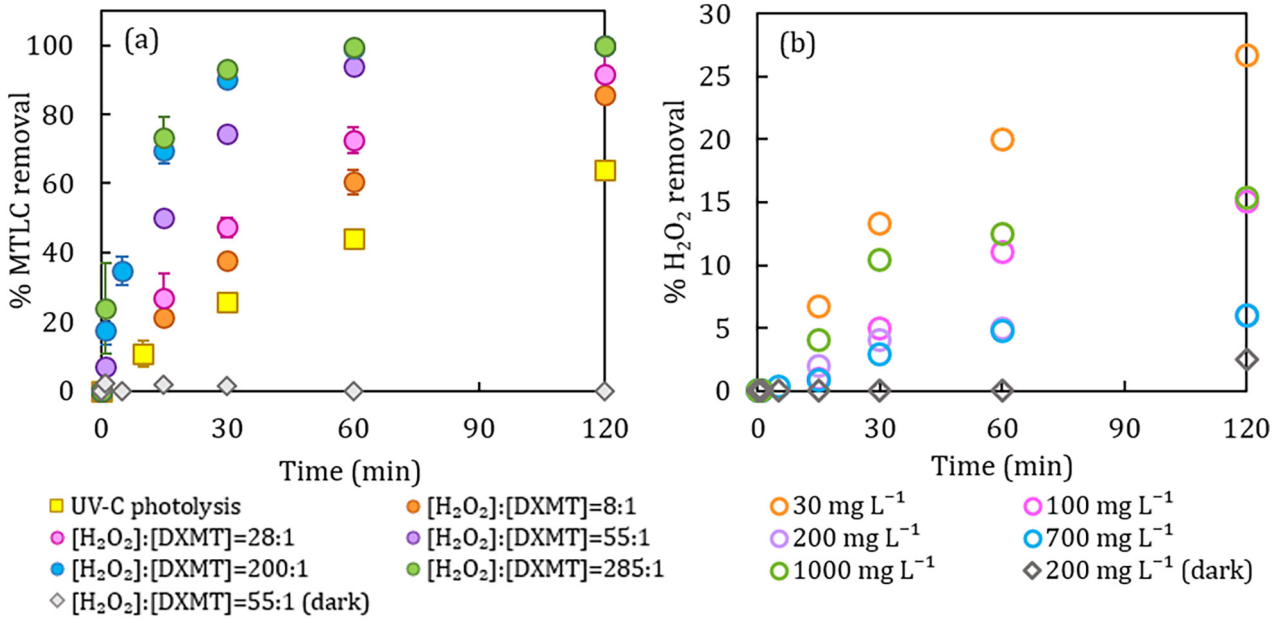


**Fig. 5.** (a) Influence of the initial concentration of hydrogen peroxide in MTLC removal by UV-C/$H_2O_2$, compared to UV-C photolysis, and (b) hydrogen peroxide consumed during the experiments. $[MTLC]_0$ = 30 mg $L^{-1}$, $[H_2O_2]_0$ = 30, 100, 200, 700, 1000 mg $L^{-1}$ corresponding to $[H_2O_2]$:[MTLC] = 8:1, 28:1, 55:1, 200:1, 285:1, UV-C irradiance = 12 W $m^{-2}$, ultrapure water, pH natural = 6, reaction volume = 0.45 L.

NaOCl experiments for the degradation of MTLC and DXMT compared to the UV-C photolysis, together with the quantification of chlorine specie. Table S.4 summarizes the kinetic results for the degradation of the target compounds with 10 mg $L^{-1}$ of NaOCl.

The addition of sodium hypochlorite to the degradation of MTLC improved by 3 % the removal with 10 mg $L^{-1}$ and by 9.5 % with 100 mg $L^{-1}$ after 30 min of reaction, taking the photolytic degradation of MTLC as benchmark (Fig. 6a). Regarding DXMT, the addition of 10 mg $L^{-1}$ of

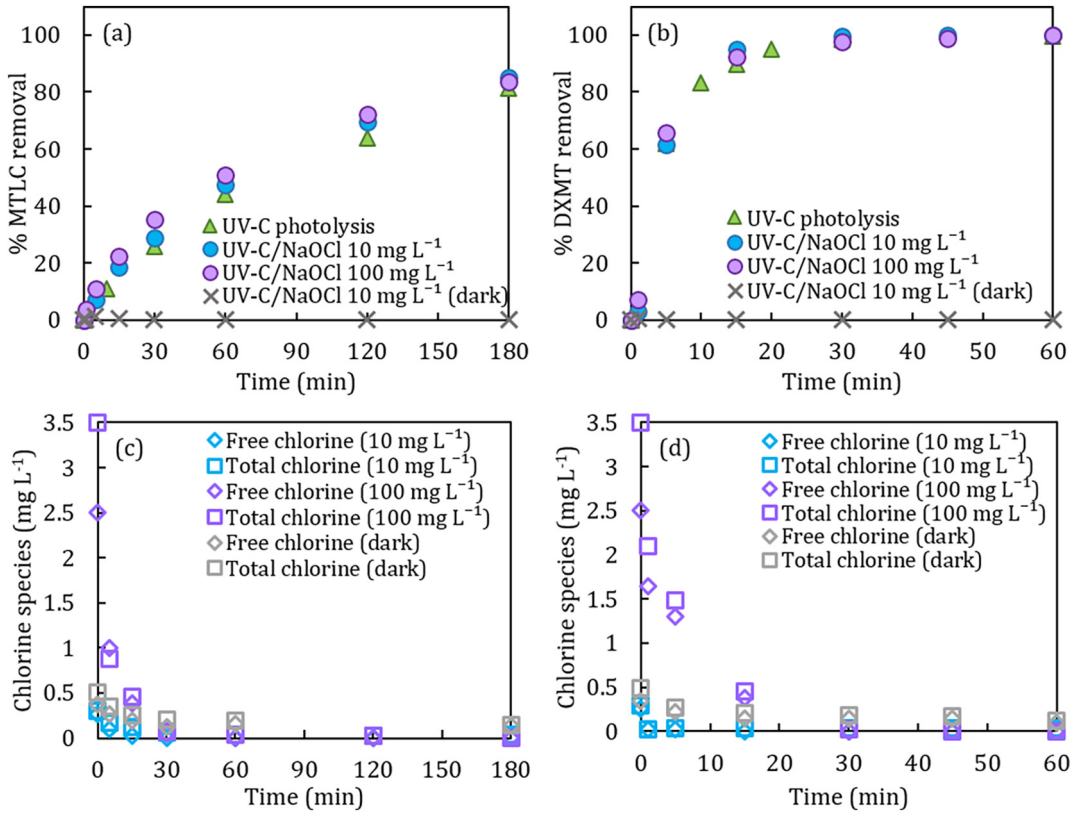


**Fig. 6.** Influence of the initial concentration of sodium hypochlorite (a) in the MTLC removal by UV-C/NaOCl, and (b) in the DXMT removal by UV-C/NaOCl, compared to UV-C photolysis and UV-C/NaOCl in dark conditions. The concentration of free chlorine (diamonds) and total chlorine (rectangles) was measured for (c) MTLC and (d) DXMT experiments. $[MTLC]_0$ = $[DXMT]_0$ = 30 mg $L^{-1}$, $[NaOCl]_0$ = 10, 100 mg $L^{-1}$ and 10 mg $L^{-1}$ under dark conditions, UV-C irradiance = 12 W $m^{-2}$, ultrapure water, pH natural = 6, reaction volume = 0.45 L.

NaOCl improved the elimination by 1.2 % with respect to UV-C photolysis, while the addition of 100 mg $L^{-1}$ of NaOCl obtained a 5.3 % of increase in the elimination after 10 min of experiment (Fig. 6b), considering the experimental error. These results confirmed that HOCl and $OCl^-$ were not able to significantly enhance the photolytic degradation of the target CECs. Some authors observed the same trend; for instance, Chaves et al. (2020) concluded that modifying the chlorine dose did not affect the degradation kinetics. Chlorine species (free chlorine and total chlorine) were measured during the experiments. Fig. 6c and d show the concentration of these species during the experiments of degradation of MTLC and DXMT, respectively. From the comparison between these data and the kinetic data shown in Fig. 6a and b the influence of chlorine species on the degradation kinetics can be deduced. Therefore, the slight increase in the elimination rate of DXMT and MTLC it is not enough for the technology to be considered an efficient alternative to promote UV-C photolysis, due to the costs of additional reagents and their subsequent removal, as it will be further confirmed.

Furthermore, the analysis of Total Organic Carbon (TOC) was performed to measure the mineralization degree for each selected UV photodegradation process. It was observed that after 120 min, the degree of DXMT mineralization was higher than that of MTLC, for the studied conditions. Nevertheless, the technology that achieved higher mineralization degrees was UV/$TiO_2$ (Fig. S.4).

### 3.3. Economic analysis

The economic analysis was carried out to assess the economic feasibility and to compare the studied processes. The economic evaluation was calculated per unit of treated volume of water (€ $m^{-3}$ of water) (Eq. (13)). The economic analysis comprises the costs of chemicals and energy. For the energy costs, the electrical energy per order ($E_{EO}$) as the energy requirements of the different processes and the electricity cost were taken into consideration (Eq. (11)). The electrical energy per order is the electric energy in kilowatt hours (kWh) required to degrade a contaminant by one order of magnitude in a unit volume of treated water (Eq. (10)) (Bolton et al., 2001). The electricity cost used was the average cost of the industrial energy in Spain at the moment of writing this article (0.076 € $kWh^{-1}$).

$$E_{EO} = \frac{P_{el} \cdot t}{V \cdot \log\left(\frac{C_0}{C_f}\right)} = \frac{P_{el} \cdot t}{V \cdot 0.434 \cdot \ln\left(\frac{C_0}{C_f}\right)} \quad (10)$$

where $P_{el}$ is the electric power (kW), t is the time (h), V is the reaction volume ($m^3$), log is the decimal logarithm, ln is the natural logarithm and $C_0$ and $C_f$ are the initial and final compound concentrations, respectively (mM).

$$Cost_{energy} = E_{EO}\ (kWh\ m^{-3}) \cdot Electricity\ cost\ (€\ kWh^{-1}) \quad (11)$$

To estimate the chemicals cost, both chemicals and their concentration were taken into account (Eq. (12)) (Goi and Trapido, 2002; Mousset et al., 2021). The cost of chemicals used was 541 € $m^{-3}$ for titanium dioxide (Chemanalyst, 2022), 502 € $m^{-3}$ for hydrogen peroxide 30 %, and 148 € $m^{-3}$ for sodium hypochlorite 10 %, for large-scale reagents as taken from the suppliers. For the photocatalysis experiments, 0.5 g $L^{-1}$ of $TiO_2$ was used at laboratory scale, but for a more realistic estimation it was assumed that the catalyst will be reused in 10 consecutive runs (Bahrudin et al., 2019).

$$Cost_{reactants} = \left(\frac{Chemicals\ cost\ (€\ kg^{-1}) \cdot Mass\ chemicals\ (kg)}{Volume\ (m^3)}\right) \quad (12)$$

$$Cost_{total} = Cost_{energy} + Cost_{reactants} \quad (13)$$

The total cost was selected to better compare the studied treatments. Tables 1 and 2 summarize the costs of the different processes in ultrapure water spiked with 30 mg $L^{-1}$ of DXMT and MTLC, respectively. Three levels of oxidant concentration are considered, low, optimal, and high, for the cost calculations. It should be noted that the costs related to labor, equipment, replacements and other operating costs are not considered in the analysis as the prices are variable and can mislead the evaluation.

Even though UV-C/NaOCl was one of the fastest treatments for the degradation of DXMT ($2.06{\cdot}10^{-1}$ $min^{-1}$ for 10 mg $L^{-1}$ and $1.99{\cdot}10^{-1}$ $min^{-1}$ for 100 mg $L^{-1}$ of NaOCl), and thus, the energy requirements are the lowest, the total cost of the process exceeds that of UV-C photolysis ($1.53{\cdot}10^{-1}$ $min^{-1}$) due to the cost of adding 10 mg $L^{-1}$ or 100 mg $L^{-1}$ of NaOCl, which represents 77 % and 97 % of the total cost, respectively. The influence of the chemicals in the total cost is incremented in the UV-C/$H_2O_2$ process because of the concentration used, the high price and the unsatisfactory degradation efficiency. The kinetic constants of UV-C/$H_2O_2$ processes are similar to the kinetic constant of UV-C photolysis ($1.56{\cdot}10^{-1}$ $min^{-1}$ with 300 mg $L^{-1}$, and $1.15{\cdot}10^{-1}$ $min^{-1}$ with 3000 mg $L^{-1}$ of $H_2O_2$) and their energy requirements are similar as well, but the cost of $H_2O_2$ addition accounts for 99 % of the total cost in both cases, increasing in 150 € $m^{-3}$ and 1506 € $m^{-3}$, respectively, the UV-C photolysis operation cost. Therefore, $H_2O_2$ posed economic and environmental issues. In photocatalysis, with UV-C and UV-A, the degradation of DXMT achieved different kinetic constants, with a 10-fold difference: $1.71{\cdot}10^{-2}$ $min^{-1}$ with UV-C and $1.52{\cdot}10^{-1}$ $min^{-1}$ with UV-A. Although this different degradation rates and the subsequent difference in the $E_{EO}$, the reagent cost accounts for 94 % and 97 % for UV-C and UV-A, respectively, achieving similar total costs. With respect to UV-C and UV-A photolysis, the kinetics are also 10-fold different despite the difference between UV-C and UV-A lamps irradiances ($1.53{\cdot}10^{-1}$ $min^{-1}$ for UV-C and $1.39{\cdot}10^{-2}$ $min^{-1}$ for UV-A), confirming that UV-A lamp performance would be even more unfavorable if carried out at the same conditions than UV-C lamp. Moreover, as the process does not need the addition of chemicals, the difference in the total cost is due to the differences in the energy requirements. Therefore, it can be highlighted that, after this study, UV-C photolysis is the most competitive process to degrade DXMT, under the optimum working conditions, in terms of kinetics, economy and energy.

Regarding MTLC degradation, as it happens for DXMT molecule, the degradation of MTLC by photocatalysis achieved kinetic constants with a 10-fold difference: $1.96{\cdot}10^{-2}$ $min^{-1}$ with UV-C and $2.62{\cdot}10^{-1}$ $min^{-1}$ with UV-A, despite the lamp irradiance differences between both lamps. Although this different degradation rates and the subsequent difference in the

**Table 1**
Costs evaluation of the different processes for the degradation of 30 mg $L^{-1}$ of DXMT in ultrapure water.

| Technology | $[H_2O_2]_0$ (kg $m^{-3}$) | $[TiO_2]_0$ (kg $m^{-3}$) | $[NaOCl]_0$ (kg $m^{-3}$) | $E_{EO}$ (kWh $m^{-3}$) | Energy cost (€ $m^{-3}$) | Reagent cost (€ $m^{-3}$) | Total cost (€ $m^{-3}$) |
|---|---|---|---|---|---|---|---|
| Photolysis UV-C | 0 | 0 | 0 | 7.83 | 1 (100 %) | 0 (0 %) | 1 |
| Photolysis UV-A | 0 | 0 | 0 | 326.60 | 25 (100 %) | 0 (0 %) | 25 |
| UV-C/$TiO_2$ | 0 | 0.05 | 0 | 69.86 | 5 (16 %) | 27 (84 %) | 32 |
| UV-A/$TiO_2$ | 0 | 0.05 | 0 | 29.79 | 2 (8 %) | 27 (92 %) | 29 |
| UV-C/$H_2O_2$ | 0.03 | 0 | 0 | 8.85 | 1 (4 %) | 15 (96 %) | 16 |
| | 0.3 | 0 | 0 | 7.66 | 1 (1 %) | 150 (99 %) | 151 |
| | 3 | 0 | 0 | 10.42 | 1 (1 %) | 1506 (99 %) | 1507 |
| UV-C/NaOCl | 0 | 0 | 0.01 | 5.79 | 1 (23 %) | 1 (77 %) | 2 |
| | 0 | 0 | 0.1 | 6.01 | 0 (3 %) | 15 (97 %) | 15 |

**Table 2**
Costs evaluation of the different processes for the degradation of 30 mg $L^{-1}$ of MTLC in ultrapure water.

| Technology | $[H_2O_2]_0$ (kg $m^{-3}$) | $[TiO_2]_0$ (kg $m^{-3}$) | $[NaOCl]_0$ (kg $m^{-3}$) | $E_{EO}$ (kWh $m^{-3}$) | Energy cost (€ $m^{-3}$) | Reagent cost (€ $m^{-3}$) | Total cost (€ $m^{-3}$) |
|---|---|---|---|---|---|---|---|
| Photolysis UV-C | 0 | 0 | 0 | 129.86 | 10 (100 %) | 0 (0 %) | 10 |
| Photolysis UV-A | 0 | 0 | 0 | 11,349.33 | 863 (100 %) | 0 (0 %) | 863 |
| UV-C/$TiO_2$ | 0 | 0.05 | 0 | 60.95 | 5 (15 %) | 27 (85 %) | 32 |
| UV-A/$TiO_2$ | 0 | 0.05 | 0 | 17.30 | 1 (5 %) | 27 (95 %) | 28 |
| UV-C/$H_2O_2$ | 0.03 | 0 | 0 | 77.07 | 6 (28 %) | 15 (72 %) | 21 |
| | 0.2 | 0 | 0 | 18.41 | 1 (1 %) | 100 (99 %) | 102 |
| | 1 | 0 | 0 | 12.68 | 1 (1 %) | 502 (99 %) | 503 |
| UV-C/NaOCl | 0 | 0 | 0.01 | 103.88 | 8 (84 %) | 1 (16 %) | 9 |
| | 0 | 0 | 0.1 | 106.67 | 8 (35 %) | 15 (65 %) | 23 |

$E_{EO}$, the reagent cost accounts for 85 % and 95 % for UV-C and UV-A, respectively, achieving similar total costs. The second fastest process is UV-C/$H_2O_2$ with 200 mg $L^{-1}$ of $H_2O_2$, obtaining the second lowest $E_{EO}$. Nevertheless, as in DXMT degradation, the cost of adding 200 mg $L^{-1}$ of $H_2O_2$ increases the cost in 92 € $m^{-3}$ with respect to UV-C photolysis (99 % of the total cost is accounted for by the chemical), becoming the less effective treatment, in terms of economy and environmental principles. UV-C/NaOCl with both concentrations is 5.5 times slower than UV-C/$H_2O_2$ and, however, the total operational cost is the lowest one due to the concentration of the oxidant used and the costs of chemicals. With respect to UV-C and UV-A photolysis, the degradation rate is very low due to the poor light absorption of the MTLC molecule under UV-C radiation and even worse under UV-A radiation ($9.20{\cdot}10^{-3}$ $min^{-1}$ for UV-C and $4.00{\cdot}10^{-4}$ $min^{-1}$ for UV-A). As photolysis does not need the addition of chemicals, the total cost varies as function of the energy requirements (which consider the kinetics). In particular, UV-C photolysis resulted in the second lowest total cost (nearly the same as the lowest) even though its kinetic rate placed the treatment for the degradation of MTLC as the second slower, only followed by UV-A photolysis. Hence, UV-C photocatalysis is the most competitive alternative for the degradation of MTLC, under the optimum working conditions, in terms of kinetics, economy and energy. Moreover, it can be highlighted that the UV-C/$H_2O_2$ process, although it achieved faster degradation, is not a suitable technology regarding economy and environmental principles. Some authors estimate the net impact of UV-C/$H_2O_2$ technology by a Life Cycle Assessment (LCA), determining that it is not an appropriate alternative from an environmental point of view (Köhler et al., 2012). Although UV-C/$H_2O_2$ was not the best option from the economic and sustainability aspects, it was demonstrated that it performs better than UV-C/peroxymonosulfate (PMS) and UV-C/persulfate (PS) in an LCA analysis (Pesqueira et al., 2022).

In the literature, Goi and Trapido (2002) achieved a cost of 61.1 € $m^{-3}$ for the photolysis of 4-nitrophenol, while other AOPs such as UV-C/$H_2O_2$, Fenton and photo-Fenton resulted in 1.22 € $m^{-3}$, 0.06 € $m^{-3}$, and 0.20 € $m^{-3}$, respectively. It is important to note that they used a low-pressure mercury lamp, with less energy requirements than the LEDs in this study, but the sustainability problems related to the lamp after use were not considered.

With this comparison, it has been demonstrated that UV-C photolysis and UV-C photocatalysis are promising alternatives for the removal of contaminants of emerging concern from treated wastewaters, depending on the chemical structure of the molecules.

There is a lack of literature references that evaluate the environmental sustainability of each process, so the electricity carbon footprint was also calculated considering the power of each lamp, the time required for the degradation of 90 % of the target compound, and the standard value of $CO_2$ emitted for the electricity in Spain in 2022 (259 g-$CO_{2\ eq}$ per kWh) (Eq. (14)). The most sustainable technology was UV-C photolysis for both micropollutants. Table S.6 details the carbon footprint values of the different technologies and compounds.

$$\text{Carbon footprint } (g - CO_2) = \left(\frac{P_{el}\ (kW) \cdot t\ (h)}{3.9}\right) \cdot 259 \quad (14)$$

Regarding the studies related to the evaluation of the carbon footprint of photo-degradation processes in the literature, Mo et al. (2018) reported a comparison of the carbon footprint and embodied energy of four different drinking water treatments: granular activated carbon filtration (GAC), ozonation, and UV-C with two different irradiation doses: 30 (UV30), and 186 mJ $cm^{-2}$ (UV186). They reported that UV30 was the second technology of embodied energy and carbon footprint, only surpassed by GAC, not included in this study. Moreover, they obtained that UV30 was the most cost-effective of the four selected treatments. McKee and Chatzisymeon (2022) identified the energy consumption as an environmental hotspot of UV photo-degradation technologies and they ranked the technologies according to the environmental sustainability as follows: solar > UV-LED > conventional lamps (McKee and Chatzisymeon, 2022).

Moreover, the UV-A and UV-C radiation of the present study has been provided by different UV LED lamps, so their efficiency is not the same. UV-C LED technology is quite novel and therefore, less efficient than conventional lamps or UV-A LED, but they potentially have much room to improve. As a comparative parameter of the efficiency, the LED energy yield is described in this work as the irradiance emitted by the LED lamp, in $W_r$ $m^{-2}$, with respect to the total energy consumption or the electric power consumed, in $W_e$. UV-A LED lamp has a LED energy yield of 28.30 $W_r$ $m^{-2}$ $W_e^{-1}$, while UV-C LED lamp has a value of LED energy yield of 0.86 $W_r$ $m^{-2}$ $W_e^{-1}$. Therefore, it can be confirmed that UV-A LED lamps are more energy efficient and because of that they have been widely studied for photo-degradation technologies. UV-C LED lamps need more investigation to improve their efficiency, due to their potential to surpass other UV lamps in terms of efficiency and lifetime.

## 4. Conclusions

Overall, this study demonstrates that the UV-C LED technology is a promising and sustainable approach for the degradation of different organic molecules, such as contaminants of emerging concern (CECs) working under irradiation dose typical of disinfection processes. This research assesses the influence of different operating parameters and different UV LED technologies in the degradation of DXMT and MTLC, which belong to the groups of pharmaceuticals and phytosanitary compounds, respectively, aiming at increasing the knowledge beyond disinfection and extending the analysis to the degradation of CECs. In UV-C photolysis, the first order kinetic constant of DXMT was higher at lower initial concentration in the range between 3 mg $L^{-1}$ (0.0076 mmol $L^{-1}$) and 30 mg $L^{-1}$ (0.076 mmol $L^{-1}$), with values of $3.15{\cdot}10^{-2}$ $min^{-1}$ and $1.60{\cdot}10^{-2}$ $min^{-1}$, respectively. The DXMT molecule is highly susceptible to degradation by UV-C photolysis and thus, when the concentration is higher, the competition for incident photons increases. However, MTLC degradation was not influenced by the initial concentration in a range from 3 mg $L^{-1}$ (0.011 mmol $L^{-1}$) to 30 mg $L^{-1}$ (0.11 mmol $L^{-1}$), with an average degradation rate constant of $7.00{\cdot}10^{-3}$ $min^{-1}$. A similar performance had been previously observed with similar molecular structures. Comparing the kinetic results in ultra-pure water and WWTP secondary effluents no effect of the water matrix was observed for the degradation of DXMT and MTLC. Similarly, the pH in a range from 3 to 10 had no influence on the degradation of both compounds, because of their $pK_a$ values.

Moreover, this investigation confirms that the photolytic mechanism in the UV range is clearly related to the chemical structure of the target molecules, which determines their light absorption. Thus, for molecules with few bonds absorbing in the UV-C wavelength range the addition of oxidants is needed. Then, other light driven AOPs, such as photocatalysis and UV/$H_2O_2$, improve the degradation of MTLC but they did not show the same influence on DXMT degradation. Regarding the degradation kinetics of each contaminant by AOPs, DXMT kinetics followed the order UV-C/NaOCl > UV-A/$TiO_2$ ≈ UV-C/$H_2O_2$ ≈ UV-C > UV-C/$TiO_2$ > UV-A, whereas for MTLC the following order was concluded UV-A/$TiO_2$ > UV-C/$H_2O_2$ > UV-C/$TiO_2$ > UV-C/NaOCl > UV-C > UV-A.

Additionally, an economic evaluation of the different technologies was carried out, and the energy, chemicals and total cost were taken into account. The total costs of the degradation of both contaminants follows the order UV-C < UV-C/NaOCl < UV-A < UV-A/$TiO_2$ ≈ UV-C/$TiO_2$ < UV-C/$H_2O_2$. Even though DXMT and MTLC have different energy requirements, the total costs revealed that the cost associated to the consumption of chemicals was predominant.

Finally, it is possible to conclude that UV-C photolysis appears as the most cost-effective and environmentally sustainable process for the degradation of persistent organic molecules and disinfection. Nevertheless, UV-C LED lamps need further investigation regarding the energy yield, to optimize the ratio of emitted irradiance to energy consumed.

## CRediT authorship contribution statement

**Deva Pelayo:** Conceptualization, Methodology, Validation, Investigation, Writing – original draft, Writing – review & editing. **María J. Rivero:** Conceptualization, Methodology, Validation, Writing – review & editing, Supervision, Resources, Project administration, Funding acquisition. **Germán Santos:** Resources, Project administration, Funding acquisition. **Pedro Gómez:** Resources, Project administration, Funding acquisition. **Inmaculada Ortiz:** Conceptualization, Methodology, Validation, Writing – review & editing, Supervision, Resources, Project administration, Funding acquisition.

## Data availability

The data that has been used is confidential.

## Declaration of Competing Interest

The authors declare that they have no known competing financial interests or personal relationships that could have appeared to influence the work reported in this paper.

## Acknowledgements

These results are part of the R&D project RTC2019-006820-5 funded by MCIN/AEI/10.13039/501100011033.

## Appendix A. Supplementary data

Supplementary data to this article can be found online at https://doi.org/10.1016/j.scitotenv.2022.161376.

## References

Bahrudin, N.N., Nawi, M.A., Nawawi, W.I., 2019. Enhanced photocatalytic decolorization of methyl orange dye and its mineralization pathway by immobilized $TiO_2$/polyaniline. Res. Chem. Intermed. 45, 2771–2795. https://doi.org/10.1007/s11164-019-03762-y.

Barquín, C., Rivero, M.J., Ortiz, I., 2022. Shedding light on the performance of magnetically recoverable $TiO_2$/$Fe_3O_4$/rGO-5 photocatalyst. Degradation of S-metolachlor as case study. Chemosphere 307, 135991. https://doi.org/10.1016/j.chemosphere.2022.135991.

Bolton, J.R., Bircher, K.G., Tumas, W., Tolman, C.A., 2001. Figures-of-merit for the technical development and application of advanced oxidation technologies for both electric- and solar-driven systems. Pure Appl. Chem. 73, 627–637. https://doi.org/10.1351/pac200173040627.

Bradley, P.M., Romanok, K.M., Duncan, J.R., Battaglin, W.A., Clark, J.M., Hladik, M.L., Huffman, B.J., Iwanowicz, L.R., Journey, C.A., Smalling, K.L., 2020. Exposure and potential effects of pesticides and pharmaceuticals in protected streams of the US National park Service southeast region. Science of the Total Environment 704, 135431. https://doi.org/10.1016/j.scitotenv.2019.135431.

Cantalupi, A., Maraschi, F., Pretali, L., Albini, A., Nicolis, S., Ferri, E.N., Profumo, A., Speltini, A., Sturini, M., 2020. Glucocorticoids in freshwaters: degradation by solar light and environmental toxicity of the photoproducts. Int. J. Environ. Res. Public Health 17, 1–15. https://doi.org/10.3390/ijerph17238717.

Cerreta, G., Roccamante, M.A., Oller, I., Malato, S., Rizzo, L., 2019. Contaminants of emerging concern removal from real wastewater by UV/free chlorine process: a comparison with solar/free chlorine and UV/$H_2O_2$ at pilot scale. Chemosphere 236, 124354. https://doi.org/10.1016/j.chemosphere.2019.124354.

Chaves, F.P., Gomes, G., Della-Flora, A., Dallegrave, A., Sirtori, C., Saggioro, E.M., Bila, D.M., 2020. Comparative endocrine disrupting compound removal from real wastewater by UV/Cl and UV/$H_2O_2$: effect of pH, estrogenic activity, transformation products and toxicity. Sci. Total Environ. 746, 141041. https://doi.org/10.1016/j.scitotenv.2020.141041.

Chemanalyst, 2022. Titanium Dioxide Price Trend and Forecast. . https://www.chemanalyst.com/Pricing-data/titanium-dioxide-52.

Choi, S.W., Shahbaz, H.M., Kim, J.U., Kim, D.H., Yoon, S., Jeong, S.H., Park, J., Lee, D.U., 2020. Photolysis and $TiO_2$ photocatalytic treatment under UVC/VUV irradiation for simultaneous degradation of pesticides and microorganisms. Appl. Sci. 10, 4493. https://doi.org/10.3390/app10134493.

Čizmić, M., Ljubas, D., Rožman, M., Ašperger, D., Ćurković, L., Babíc, S., 2019. Photocatalytic degradation of azithromycin by nanostructured $TiO_2$ film: kinetics, degradation products, and toxicity. Materials 12, 873. https://doi.org/10.3390/ma12060873.

Collivignarelli, C., Sorlini, S., 2004. AOPs with ozone and UV radiation in drinking water: contaminants removal and effects on disinfection byproducts formation. Water Sci. Technol. 49 (4), 51–56. https://doi.org/10.2166/wst.2004.0218.

Costa, E.P., Roccamante, M., Plaza-Bolaños, P., Oller, I., Agüera, A., Amorim, C.C., Malato, S., 2021. Aluminized surface to improve solar light absorption in open reactors: application for micropollutants removal in effluents from municipal wastewater treatment plants. Sci. Total Environ. 755, 142624. https://doi.org/10.1016/j.scitotenv.2020.142624.

Diamanti, K.S., Alygizakis, N.A., Nika, M.C., Oswaldova, M., Oswald, P., Thomaidis, N.S., Slobodnik, J., 2020. Assessment of the chemical pollution status of the Dniester River basin by wide-scope target and suspect screening using mass spectrometric techniques. Anal. Bioanal. Chem. 412, 4893–4907. https://doi.org/10.1007/s00216-020-02648-y.

Dimou, A.D., Sakkas, V.A., Albanis, T.A., 2005. Metolachlor photodegradation study in aqueous media under natural and simulated solar irradiation. J. Agric. Food Chem. 53, 694–701. https://doi.org/10.1021/jf048766w.

Dominguez, S., Rivero, M.J., Gomez, P., Ibañez, R., Ortiz, I., 2016. Kinetic modeling and energy evaluation of sodium dodecylbenzenesulfonate photocatalytic degradation in a new LED reactor. J. Ind. Eng. Chem. 37, 237–242. https://doi.org/10.1016/j.jiec.2016.03.031.

Drugbank, 2022. Dexamethasone. . https://go.drugbank.com/drugs/DB01234.

Escudero, C.J., Iglesias, O., Dominguez, S., Rivero, M.J., Ortiz, I., 2017. Performance of electrochemical oxidation and photocatalysis in terms of kinetics and energy consumption. New insights into the p-cresol degradation. J. Environ. Manag. 195, 117–124. https://doi.org/10.1016/j.jenvman.2016.04.049.

Escudero, J., Muñoz, J.L., Morera-Herreras, T., Hernandez, R., Medrano, J., Domingo-Echaburu, S., Barceló, D., Orive, G., Lertxundi, U., 2021. Antipsychotics as environmental pollutants: an underrated threat? Sci. Total Environ. 769, 144634. https://doi.org/10.1016/j.scitotenv.2020.144634.

Fan, L., Wang, J., Huang, Y., Su, L., Li, C., Zhao, Y.H., Martyniuk, C.J., 2022. Comparative analysis on the photolysis kinetics of four neonicotinoid pesticides and their photo-induced toxicity to vibrio fischeri: pathway and toxic mechanism. Chemosphere 287, 132303. https://doi.org/10.1016/j.chemosphere.2021.132303.

Farkas, J., Náfrádi, M., Hlogyik, T., Cora Pravda, B., Schrantz, K., Hernádi, K., Alapi, T., 2018. Comparison of advanced oxidation processes in the decomposition of diuron and monuron-efficiency, intermediates, electrical energy per order and the effect of various matrices. Environ. Sci.: Water Res. Technol. 4, 1345–1360. https://doi.org/10.1039/c8ew00202a.

Ferhi, S., Vieillard, J., Garau, C., Poultier, O., Demey, L., Beaulieu, R., Penalva, P., Gobert, V., Portet-Koltalo, F., 2021. Pilot-scale direct UV-C photodegradation of pesticides in groundwater and recycled wastewater for agricultural use. J. Environ. Chem. Eng. 9, 106120. https://doi.org/10.1016/j.jece.2021.106120.

Ferreira, L.C., Fernandes, J.R., Rodríguez-Chueca, J., Peres, J.A., Lucas, M.S., Tavares, P.B., 2020. Photocatalytic degradation of an agro-industrial wastewater model compound using a UV LEDs system: kinetic study. J. Environ. Manag. 269, 110740. https://doi.org/10.1016/j.jenvman.2020.110740.

Goi, A., Trapido, M., 2002. Hydrogen peroxide photolysis, Fenton reagent and photo-Fenton for the degradation of nitrophenols: a comparative study. Chemosphere 46, 913–922. https://doi.org/10.1016/S0045-6535(01)00203-X.

Guelfi, D.R.V., Gozzi, F., Machulek, A., Sirés, I., Brillas, E., de Oliveira, S.C., 2018. Degradation of herbicide S-metolachlor by electrochemical AOPs using a boron-doped diamond anode. Catal. Today 313, 182–188. https://doi.org/10.1016/j.cattod.2017.10.026.

Hansen, M., Thomson, G.D., Lee, K., Nubbe, V., Pattison, M., 2021. DOE Lighting R&D Program, "Germicidal Ultraviolet Lighting R&D Meeting.". U.S. Department of Energy, Office of Energy Efficiency and Renewable Energy.

Hildebrandt, A., Lacorte, S., Barceló, D., 2007. Assessment of priority pesticides, degradation products, and pesticide adjuvants in groundwaters and top soils from agricultural areas of the Ebro river basin. Anal. Bioanal. Chem. 387, 1459–1468. https://doi.org/10.1007/s00216-006-1015-z.

Hildebrandt, A., Guillamón, M., Lacorte, S., Tauler, R., Barceló, D., 2008. Impact of pesticides used in agriculture and vineyards to surface and groundwater quality (North Spain). Water Res. 42, 3315–3326. https://doi.org/10.1016/j.watres.2008.04.009.

Hurwitz, G., Pornwongthong, P., Mahendra, S., Hoek, E.M.V., 2014. Degradation of phenol by synergistic chlorine-enhanced photo-assisted electrochemical oxidation. Chem. Eng. J. 240, 235–243. https://doi.org/10.1016/j.cej.2013.11.087.

Kalisvaart, B.F., 2001. Photobiological effects of polychromatic medium pressure UV lamps. Water Sci. Technol. 43 (4), 191–197. https://doi.org/10.2166/wst.2001.0219.

Kalisvaart, B.F., 2004. Re-use of wastewater: preventing the recovery of pathogens by using medium-pressure UV lamp technology. Water Sci. Technol. 50 (6), 337–344. https://doi.org/10.2166/wst.2004.0393.

Khan, J.A., He, X., Shah, N.S., Sayed, M., Khan, H.M., Dionysiou, D.D., 2017. Degradation kinetics and mechanism of desethyl-atrazine and desisopropyl-atrazine in water with ·OH and $SO_4^{\cdot-}$ based-AOPs. Chem. Eng. J. 325, 485–494. https://doi.org/10.1016/j.cej.2017.05.011.

Klavarioti, M., Mantzavinos, D., Kassinos, D., 2009. Removal of residual pharmaceuticals from aqueous systems by advanced oxidation processes. Environ. Int. 35, 402–417. https://doi.org/10.1016/j.envint.2008.07.009.

Köck-Schulmeyer, M., Ginebreda, A., Petrovic, M., Giulivo, M., Aznar-Alemany, Ò., Eljarrat, E., Valle-Sistac, J., Molins-Delgado, D., Diaz-Cruz, M.S., Monllor-Alcaraz, L.S., Guillem-Argiles, N., Martínez, E., Llorca, M., Farré, M., Peña, J.M., Mandaric, L., Pérez, S., Majone, B., Miren, L.de A., Barceló, D., 2021. Priority and emerging organic microcontaminants in three Mediterranean river basins: occurrence, spatial distribution, and identification of river basin specific pollutants. Science of the Total Environment 754. https://doi.org/10.1016/j.scitotenv.2020.142344.

Köhler, C., Venditti, S., Igos, E., Klepiszewski, K., Benetto, E., Cornelissen, A., 2012. Elimination of pharmaceutical residues in biologically pre-treated hospital wastewater using advanced UV irradiation technology: a comparative assessment. J. Hazard. Mater. 239–240, 70–77. https://doi.org/10.1016/j.jhazmat.2012.06.006.

Liang, H.Chao, Li, X.Zhong, Yang, Y.Hua, Sze, K.Hung, 2010. Comparison of the degradations of diphenamid by homogeneous photolysis and heterogeneous photocatalysis in aqueous solution. Chemosphere 80, 366–374. https://doi.org/10.1016/j.chemosphere.2010.04.054.

Liu, D., Song, K., Xie, G., Li, L., 2020. MBR-UV/$Cl_2$ system in treating polluted surface water with typical PPCP contamination. Sci. Rep. 10, 8835. https://doi.org/10.1038/s41598-020-65845-w.

Liu, W., Yao, H., Xu, W., Liu, G., Wang, X., Tu, Y., Shi, P., Yu, N., Li, A., Wei, S., 2020. Suspect screening and risk assessment of pollutants in the wastewater from a chemical industry park in China. Environ. Pollut. 263, 114493. https://doi.org/10.1016/j.envpol.2020.114493.

Lui, G.Y., Roser, D., Corkish, R., Ashbolt, N.J., Stuetz, R., 2016. Point-of-use water disinfection using ultraviolet and visible light-emitting diodes. Sci. Total Environ. 553, 626–635. https://doi.org/10.1016/j.scitotenv.2016.02.039.

Malvestiti, J.A., Dantas, R.F., 2019. Influence of industrial contamination in municipal secondary effluent disinfection by UV/$H_2O_2$. Environ. Sci. Pollut. Res. 26, 13286–13298. https://doi.org/10.1007/s11356-019-04705-1.

Markic, M., Cvetnic, M., Ukic, S., Kusic, H., Bolanca, T., Bozic, A.L., 2018. Influence of process parameters on the effectiveness of photooxidative treatment of pharmaceuticals. J. Environ. Sci. Health A Tox. Hazard. Subst. Environ. Eng. 53 (4), 338–351. https://doi.org/10.1080/10934529.2017.1401394.

Marson, E.O., Paniagua, C.E.S., Costa-Serge, N.M., Sousa, R.M.F., Silva, G.D., Becker, R.W., Sirtori, C., Starling, M.C.V.M., Carvalho, S.R., Trovó, A.G., 2021. Chemical and toxicological evaluation along with unprecedented transformation products during photolysis and heterogeneous photocatalysis of chloramphenicol in different aqueous matrices. Environ. Sci. Pollut. Res. 28, 23582–23594. https://doi.org/10.1007/s11356-020-09756-3.

Masschelein, W.J., 2002. UltravioletLight in Water and Wastewater Sanitation. Lewis Publishers.

Matafonova, G., Batoev, V., 2022. Dual-wavelength light radiation for synergistic water disinfection. Sci. Total Environ. 806, 151233. https://doi.org/10.1016/j.scitotenv.2021.151233.

McKee, S.M., Chatzisymeon, E., 2022. Assessing the environmental sustainability of light emitting diodes and conventional blacklight lamps for the treatment of bisphenol-a in water. Environ. Impact Assess. Rev. 97, 106886. https://doi.org/10.1016/j.eiar.2022.106886.

Mermana, J., Sutthivaiyakit, P., Blaise, C., Gagné, F., Charnsethikul, S., Kidkhunthod, P., Sutthivaiyakit, S., 2017. Photocatalysis of S-metolachlor in aqueous suspension of magnetic cerium-doped m$TiO_2$ core–shell under simulated solar light. Environ. Sci. Pollut. Res. 24, 4077–4092. https://doi.org/10.1007/s11356-016-8151-6.

Mo, W., Cornejo, P.K., Malley, J.P., Kane, T.E., Collins, M.R., 2018. Life cycle environmental and economic implications of small drinking water system upgrades to reduce disinfection byproducts. Water Res. 143, 155–164. https://doi.org/10.1016/j.watres.2018.06.047.

Mousset, E., Loh, W.H., Lim, W.S., Jarry, L., Wang, Z., Lefebvre, O., 2021. Cost comparison of advanced oxidation processes for wastewater treatment using accumulated oxygen-equivalent criteria. Water Res. 200. https://doi.org/10.1016/j.watres.2021.117234.

Neghi, N., Kumar, M., 2017. Performance analysis of photolytic, photocatalytic, and adsorption Systems in the Degradation of metronidazole on the perspective of removal rate and energy consumption. Water Air Soil Pollut. 228, 339. https://doi.org/10.1007/s11270-017-3532-0.

Ngumba, E., Gachanja, A., Tuhkanen, T., 2020. Removal of selected antibiotics and antiretroviral drugs during post-treatment of municipal wastewater with UV, UV/chlorine and UV/hydrogen peroxide. Water Environ. J. 34, 692–703. https://doi.org/10.1111/wej.12612.

Nosaka, Y., Nosaka, A.Y., 2017. Generation and detection of reactive oxygen species in photocatalysis. Chem. Rev. 117, 11302–11336. https://doi.org/10.1021/acs.chemrev.7b00161.

Office of Energy Efficiency and Renewable Energy, 2022. LED basics. https://www.energy.gov/eere/ssl/led-basics.

Olatunde, O.C., Kuvarega, A.T., Onwudiwe, D.C., 2020. Photo enhanced degradation of contaminants of emerging concern in waste water. Emerging Contaminants 6, 283–302. https://doi.org/10.1016/j.emcon.2020.07.006.

Ou, H., Ye, J., Ma, S., Wei, C., Gao, N., He, J., 2016. Degradation of ciprofloxacin by UV and UV/$H_2O_2$ via multiple-wavelength ultraviolet light-emitting diodes: effectiveness, intermediates and antibacterial activity. Chem. Eng. J. 289, 391–401. https://doi.org/10.1016/j.cej.2016.01.006.

Pariente, M.I., Segura, Y., Álvarez-Torrellas, S., Casas, J.A., de Pedro, Z.M., Diaz, E., García, J., López-Muñoz, M.J., Marugán, J., Mohedano, A.F., Molina, R., Munoz, M., Pablos, C., Perdigón-Melón, J.A., Petre, A.L., Rodríguez, J.J., Tobajas, M., Martínez, F., 2022. Critical review of technologies for the on-site treatment of hospital wastewater: from conventional to combined advanced processes. J. Environ. Manag. 320, 115769. https://doi.org/10.1016/j.jenvman.2022.115769.

Parra-Saldivar, R., Castillo-Zacarías, C., Bilal, M., Iqbal, H.M.N., Barceló, D., 2021. Sources of pharmaceuticals in water. Handbook of Environmental Chemistry 103, 33–47. https://doi.org/10.1007/698_2020_623.

Pesqueira, J.F.J.R., Marugán, J., Pereira, M.F.R., Silva, A.M.T., 2022. Selecting the most environmentally friendly oxidant for UVC degradation of micropollutants in urban wastewater by assessing life cycle impacts: hydrogen peroxide, peroxymonosulfate or persulfate? Sci. Total Environ. 808, 152050. https://doi.org/10.1016/j.scitotenv.2021.152050.

Quaresma, A.V., Rubio, K.T.S., Taylor, J.G., Sousa, B.A., Silva, S.Q., Werle, A.A., Afonso, R.J.C.F., 2021. Removal of dexamethasone by oxidative processes: structural characterization of degradation products and estimation of the toxicity. J. Environ. Chem. Eng. 9, 106884. https://doi.org/10.1016/j.jece.2021.106884.

Rancaño, L., Rivero, M.J., Mueses, M.Á., Ortiz, I., 2021. Comprehensive kinetics of the photocatalytic degradation of emerging pollutants in a led-assisted photoreactorS-metolachlor as case study. Catalysts 11, 48. https://doi.org/10.3390/catal11010048.

Raschitor, A., Romero, A., Sanches, S., Pereira, V.J., Crespo, J.G., Llanos, J., 2021. Degradation of neonicotinoids and caffeine from surface water by photolysis. Molecules 26, 7277. https://doi.org/10.3390/molecules26237277.

Rasolevandi, T., Naseri, S., Azarpira, H., Mahvi, A.H., 2019. Photo-degradation of dexamethasone phosphate using UV/Iodide process: kinetics, intermediates, and transformation pathways. J. Mol. Liq. 295, 111703. https://doi.org/10.1016/j.molliq.2019.111703.

Rathnayake, B., Heponiemi, A., Huovinen, M., Ojala, S., Pirilä, M., Loikkanen, J., Azalim, S., Saouabe, M., Brahmi, R., Vähäkangas, K., Lassi, U., Keiski, R.L., 2020. Photocatalysis and catalytic wet air oxidation: degradation and toxicity of bisphenol a containing wastewaters. Environ. Technol. 41 (25), 3272–3283. https://doi.org/10.1080/09593330.2019.1604817.

Reusch, William, Clark, J., 2020. Spectroscopy, pp. 410–427.

Ribao, P., Corredor, J., Rivero, M.J., Ortiz, I., 2019. Role of reactive oxygen species on the activity of noble metal-doped $TiO_2$ photocatalysts. J. Hazard. Mater. 372, 45–51. https://doi.org/10.1016/j.jhazmat.2018.05.026.

Sakkas, V.A., Arabatzis, I.M., Konstantinou, I.K., Dimou, A.D., Albanis, T.A., Falaras, P., 2004. Metolachlor photocatalytic degradation using $TiO_2$ photocatalysts. Appl. Catal. B Environ. 49, 195–205. https://doi.org/10.1016/j.apcatb.2003.12.008.

Sánchez-Montes, I., Salmerón García, I., Rivas Ibañez, G., Aquino, J.M., Polo-López, M.I., Malato, S., Oller, I., 2020. UVC-based advanced oxidation processes for simultaneous removal of microcontaminants and pathogens from simulated municipal wastewater at pilot plant scale. Environ. Sci.: Water Res. Technol. 6, 2553–2566. https://doi.org/10.1039/d0ew00279h.

Serra-Compte, A., Pikkemaat, M.G., Elferink, A., Almeida, D., Diogène, J., Campillo, J.A., Llorca, M., Álvarez-Muñoz, D., Barceló, D., Rodríguez-Mozaz, S., 2021. Combining an effect-based methodology with chemical analysis for antibiotics determination in wastewater and receiving freshwater and marine environment. Environ. Pollut. 271. https://doi.org/10.1016/j.envpol.2020.116313.

Silva, M.P., dos Santos Batista, A.P., Borrely, S.I., Silva, V.H.O., Teixeira, A.C.S.C., 2014. Photolysis of atrazine in aqueous solution: role of process variables and reactive oxygen species. Environ. Sci. Pollut. Res. 21, 12135–12142. https://doi.org/10.1007/s11356-014-2881-0.

Solaun, O., Rodríguez, J.G., Menchaca, I., López-García, E., Martínez, E., Zonja, B., Postigo, C., López de Alda, M., Barceló, D., Borja, Á., Manzanos, A., Larreta, J., 2021. Contaminants of emerging concern in the basque coast (N Spain): occurrence and risk assessment for a better monitoring and management decisions. Sci. Total Environ. 765, 142765. https://doi.org/10.1016/j.scitotenv.2020.142765.

Solís, R.R., Dinc, Ö., Fang, G., Nadagouda, M.N., Dionysiou, D.D., 2021. Activation of inorganic peroxides with magnetic graphene for the removal of antibiotics from wastewater. Environ. Sci. Nano 8, 960–977. https://doi.org/10.1039/d0en01280g.

Souissi, Y., Bouchonnet, S., Bourcier, S., Kusk, K.O., Sablier, M., Andersen, H.R., 2013. Identification and ecotoxicity of degradation products of chloroacetamide herbicides from UV-treatment of water. Sci. Total Environ. 458–460, 527–534. https://doi.org/10.1016/j.scitotenv.2013.04.064.

Stankov, V., Stankov, M.N., Cvetnić, M., Sigurnjak Bureš, M., Ukić, Š., Kučić Grgić, D., Lončarić Božić, A., Kušić, H., Bolanča, T., 2021. Environmental aspects of UV-C-based processes for the treatment of oxytetracycline in water. Environ. Pollut. 277, 116797. https://doi.org/10.1016/j.envpol.2021.116797.

Szeto, W., Yam, W.C., Huang, H., Leung, D.Y.C., 2020. The efficacy of vacuum-ultraviolet light disinfection of some common environmental pathogens. BMC Infect. Dis. 20 (127), 1–9. https://doi.org/10.1186/s12879-020-4847-9.

Tai, C., Peng, J.F., Liu, J.F., Jiang, G.Bin, Zou, H., 2004. Determination of hydroxyl radicals in advanced oxidation processes with dimethyl sulfoxide trapping and liquid chromatography. Anal. Chim. Acta 527, 73–80. https://doi.org/10.1016/j.aca.2004.08.019.

Wu, C., Shemer, H., Linden, K.G., 2007. Photodegradation of metolachlor applying UV and UV/$H_2O_2$. J. Agric. Food Chem. 55, 4059–4065. https://doi.org/10.1021/jf0635762.